International Journal of Concrete Structures and Materials

RESEARCH   **Open Access**

Percolation-Based Image Processing for the Plastic Viscosity of Cementitious Mortar with Super Absorbent Polymer

Asghar Aryanfar[1,2*] , Irem Şanal[2] and Jaime Marian[3]

Abstract

Super absorbent polymers (SAP) are the recent promising chemical admixtures with the potential for reducing the shrinkage, cracking, freeze/thaw and increasing the durability of the concrete. These polymers are classified as hydrogels when cross-linked and can retain exceptionally high amount of liquid solutions of their own weight. In this paper, the flowability of the concrete is quantified by means of developing a percolation-based image processing method and the transient behavior of the viscosity of the SAP-contained mortar mixture is characterized via numerical solution of Navier–Stokes relationship. In addition, rheological measurements and the analytical development has been carried out for complementary verification of the viscosity trends. Controlling the flow within such relatively short period of time is essential for tuning the functionality of concrete during the construction as well as it's respective resilience during the extended period of application.

1 Introduction

One of the most important developments in concrete technology is to control the amount of water absorbed and maintained in the concrete mix Paiva et al. (2009). Superabsorbent polymers (SAP) are new, very promising multipurpose chemical admixtures for applications in concrete with a wide window of potential for innovation. SAPs can trap water within up to ~ 100 times of their own weight Esteves (2011), change the rheological properties of fresh concrete mixture Paiva et al. (2009) and tune it's autogenous and plastic shrinkage behavior during both fresh and hardened states through internal curing Shen et al. (2015); Pang et al. (2011); Al-Nasra and Daoud (2013). Such utilization as a self-curing agent saves water as the concrete dries to a large extent Lee et al. (2016); Justs et al. (2015); Mechtcherine and Reinhardt (2012). Typical chemical composition is sodium

salt of poly-acrylate acid $[-CH_2 - CH(CO_2Na)-]_n$, a crystal-like structure classified hydrogel when cross-linked Mejlhede Jensen (2013). SAPs are commonly used in diapers, sanitary napkins, biomedical purposes, agriculture etc.

The recent introduction of SAPs into concrete has lead to promising results in terms of physical and mechanical properties which directly affect pumping, placement and compressibility of the mortar as well as the corresponding reliability in both fresh and hardened states. During absorption, water is entrained and cured into the concrete leading to hydration. Subsequently, SAP particles can slowly release their inner water as humidity supply when decreased in cement paste. This process fills the pores and reduces the micro-cracks, relieving the autogenous and drying shrinkages Wang et al. (2009). Therefore, the release process of water as well as its magnitude is a critical parameter for investigation of internal curing and it can control pumping, placement and compressibility Han et al. (2014). Additionally, predicting and controlling the workability of SAP modified concretes during the mixing process is a significant factor for the practical use

*Correspondence: aryanfar@caltech.edu
2 Bahçeşehir University, 4 Çırağan Cad, Beşiktaş, Istanbul 34353, Turkey
Full list of author information is available at the end of the article

Aryanfar *et al. Int J Concr Struct Mater*   (2021) 15:25

Page 2 of 9

of SAP in concrete industry, which dramatically changes the workability of the cement mortar samples Mechtcherine et al. (2015); Toledo Filho et al. (2012); AzariJafari et al. (2016).

Studies have shown that the addition of 0.4% of a certain type of SAP relative to cement mass will lead to a decreasing of the w/c of 0.06, causing the increase in the yield stress and the plastic viscosity Jensen and Hansen (2001). Consequently, adding a certain amount of SAP additive per cement mass is equivalent to removing water from the concrete mix due to its high water absorbency. If extra water is not added to concrete mix to compensate for absorbed water, it is inevitable to observe an increase in the yield stress and plastic viscosity of cement mortar mixtures Jensen and Hansen (2002). As the result, a decrease in slump flow spread and an increase in flow time is observed.

According to the findings of previous studies, the utilization of SAP could increase or a decrease the mechanical performance of concrete based on the type of SAP and the amount of added water, which control the workability and the mixing procedure. The flexural and compressive strength typically reduce Mechtcherine et al. (2006); Craeye and De Schutter (2008); Igarashi and Watanabe (2006). The water-entrained concrete mixes with SAP inclusion has macro-pores added, which are expected to reduce the compressive strength, albeit the self-curing SAP particles, improve continuous hydration, leading to later increase in the ultimate compressive strength. It is known that a 1% increase in voids in the concrete, reduce the compressive strength up to 5% Popovics (1998). Such marginal reduction due to macropores suggest the efficacy of SAP when utilized in their maximum capacity. In particular, at a high water-to-binder ratio ($\frac{w}{b} > 0.45$), SAP addition affect the hydration negligibly and, therefore, reduces compressive strength. Vice versa at lower ratios ($\frac{w}{b} > 0.45$), SAP addition may increase the compressive strength Powers and Brownyard (1946).

In addition to water-binding effect, it is believed that a further increase in yield stress and plastic viscosity is achievable by the inclusion of the swollen SAP particles. The absorption of water and moisture from the fresh concrete mix reduces the slump of the concrete decreasing the workability and the water needed for curing Dudziak and Mechtcherine (2010). Therefore, internal curing water is needed to compensate the moisture absorbed via SAP, where the reduction of workability can be compensated up to an extent Schröfl et al. (2012). The SAP particles create voids in the hardened cement paste (HCP) when water is released for internal curing. The formed porous concrete reduces the resulting concrete strength

KONG and ZHANG (2013, 2014). Nevertheless, very few results are available regarding the influence of SAP on the workability of concrete.

The main objective of this study is to characterize the fresh state performance of SAP-modified cementitious composites and particularly to propose an percolation-based image analysis for predicting the workability of the mortar mixtures before the casting process. For characterizing the transient behavior, the radial propagation of slump samples of mortar mixtures is measured and is correlated to the instantaneous viscosity $\mu(t)$. Hence this method introduces a cost-effective method in the absence of the advanced and costly measurement devices such as the Rheometer. Additionally this method explains rather a time-dependent viscosity, which addresses both transient and steady-state behavior of the cementitious composite during the casting process. Such depiction allows the prediction and control the workability and plastic behavior during concrete casting.

2 Methodology
2.1 Materials and Design
A simple hydration test on mixing the water with the SAP shows that it can absorb up to $100g$ of water per gram of SAP. The SAP particles grow in volume, similar to the air entrainment technique utilized for improving the resistance of concrete to the freeze–thaw. The entrainment is homogenous and enhances hydration and hardening of concrete Jensen and Hansen (2002).

The control mixture with the water-to-cement ratio of $w/c = 0.4$ was prepared as reference. The additional *SAP* content is equivalent to removing water from the concrete mixture Paiva et al. (2006), which causes the thickening of the concrete paste, decreasing the flowability and increasing the rheological results. For *SAP* contents varying between 0.3% and 0.4% , related to the mass of cement, additional water of 0.04% to 0.07% needs to be added, relative to the mass of cement Dudziak and Mechtcherine (2009). Subsequently, the mixtures were papered by varying amounts of SAP-to-cement mass containments. Additional 0.01% water for each 0.1% of SAP (both by mass of cement) was added to compensate for the absorption of mixing water by the polymers and to create mixtures showing a similar workability to the reference with a water-to-cement ratio of 0.40. Such water allowance has previously been utilized to compensate the loss of the workability Mechtcherine et al. (2006).

A maximum aggregate size of $2mm$ for the fine aggregates of ordinary Portland cement with the grade $CEM|42.5$. The mortar samples were prepared in the room with temperature of 20 ± 2^{oC}, by mixing the solid powder with liquid for $2min$ at low speed of $140 \pm 5rev/min$ and a further 2 min at high speed of

$285 \pm 10 rev/min$. The SAPs was treated by sieves, and the SAP with particle size of $150 - -200 \mu m$ was selected. The detailed properties of SAP used in this study is given in Table 1. The tea-bag test method, as suggested by RILEM, was carried out for the experimental measurements of SAP absorption–desorption. The test was applied in the cement slurry solution using an ordinary tea-bag which is filled with SAP particles and immersed in the pure water.

The mini slump flow was carried out by placing the cone in the middle of a flat piece of square glass and filled with mortar. The cone is then quickly lifted, allowing the mortar to flow. After certain enlargement the sample turns to steady shape. High resolution digital images ($15 frames/second$) were also taken at regular time intervals during the mini slump flow test to evaluate the flow behavior of materials in the subsequent computations.

2.2 Image Processing

Subsequently, an original image processing percolation-based numerical method was developed and carried out based on the flowchart presented in Fig. 1. The detailed steps are described as below.

1. The bare images Im_k from the concrete, sample of which is given in Fig. 2a contains information from the red, green and blue values (i.e., $\{R, G, B\} \in [0, 255]$) which can be transferred to a normalized gray-scale intensity image by averaging as

$$I_{i,j} = \frac{R_{i,j} + G_{i,j} + B_{i,j}}{3 \times 255} \tag{1}$$

where the $0 \le I_{i,j} \le 1$ is the intensity value of the obtained grayscale image. The concrete regions can be distinguished by establishing a grayness threshold, $I_c \in [0, 1]$, which classifies the elements into black and white classes $\{B, W\} \in (0, 1)$. This value is determined iteratively from Otsu's method by minimizing the intra-class variance σ^2 as follows Otsu (1975); Aryanfar et al. (2019): minimize σ^2, such that

Table 1 Properties of SAP-contained mortar mixtures.

$\rho_{cement}(kg/m^3)$	$d_{particle}(\mu m)$	Absorption (g/g)	Desorption (%)	SAP content
1310	150 − 200	100	5	{0, 0.2, 0.4, 0.6, 0.8}%
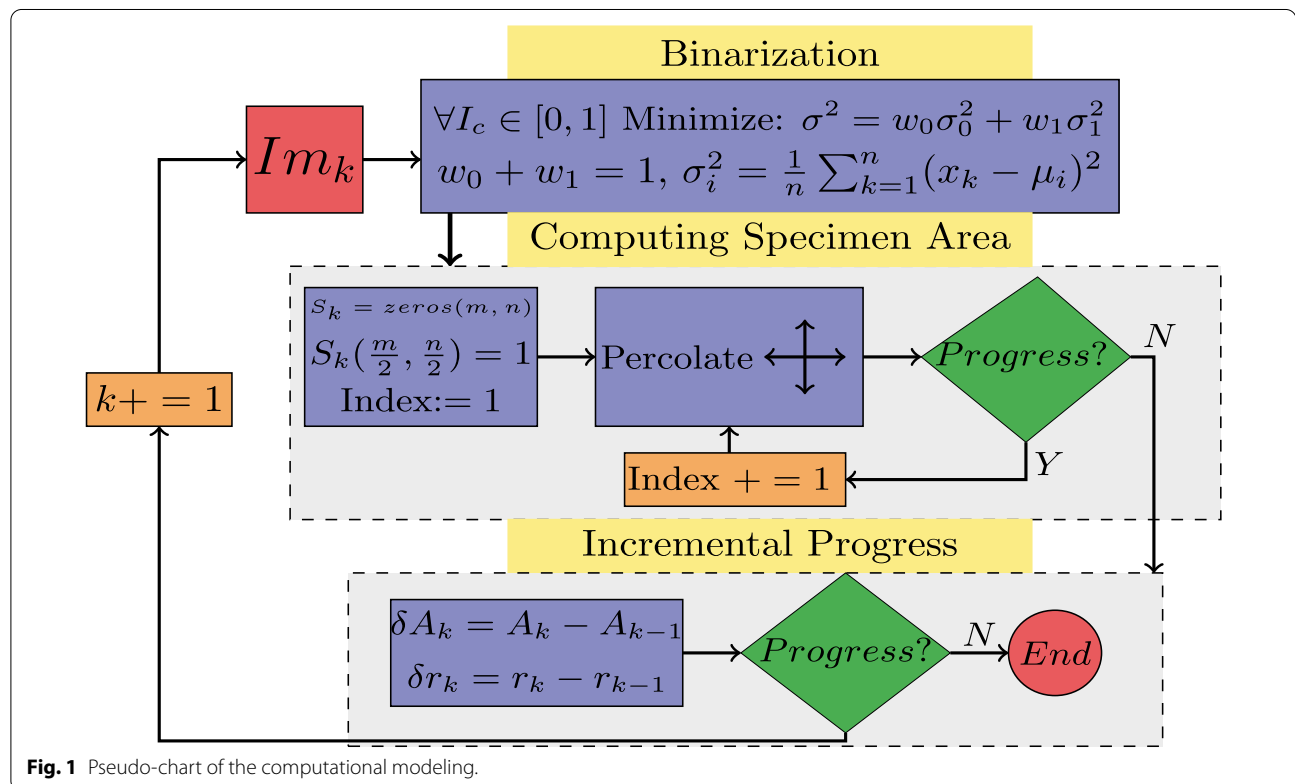
Fig. 1 Pseudo-chart of the computational modeling.

a Slump test.   **b** Image processing.

Fig. 2 Analysis.
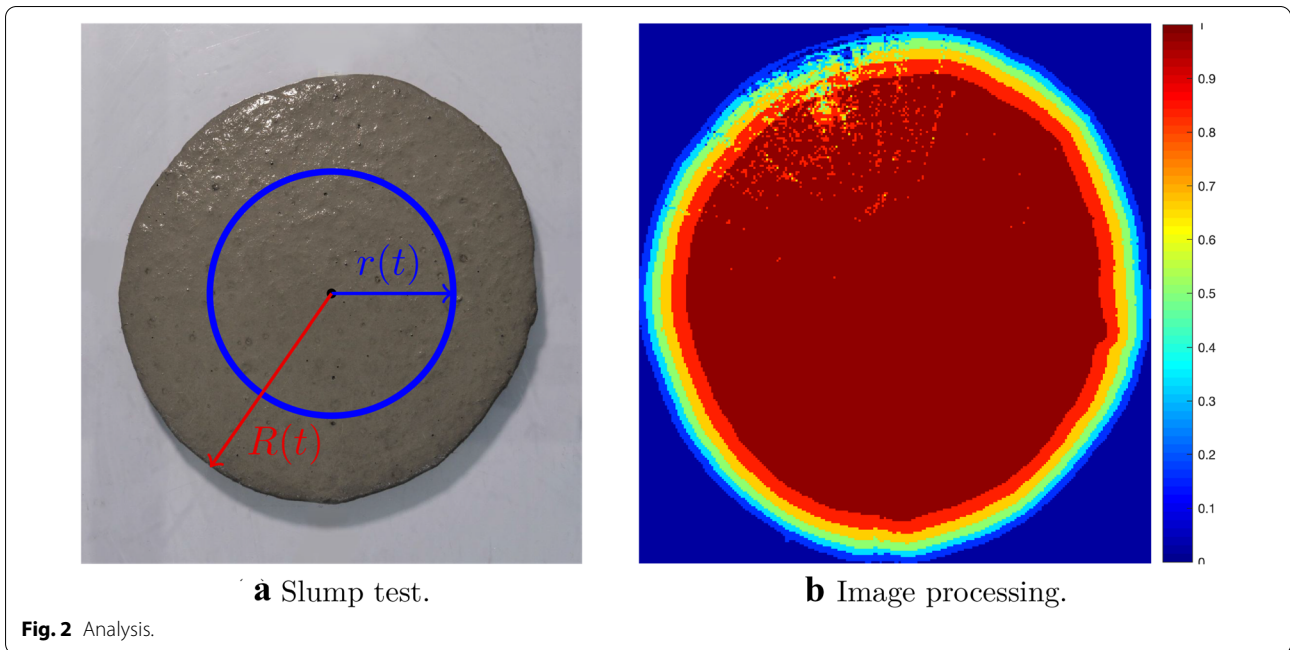
$$\begin{cases} \sigma^2 = \omega_0\sigma_0^2 + \omega_1\sigma_1^2 \\ \omega_0 + \omega_1 = 1 \end{cases} \tag{2}$$

where ω_0 and ω_1 are the fractions of black/white portions and σ_0^2 and σ_1^2 are the corresponding variances for each classified zone. The obtained binarized image from the minimization of intra-class variance σ^2 ensures the closest proximity in the values of each chosen group (*B&W*), and therefore, it ensures the best approximation of the original gray-scale image.

2. Starting from the center of each image in the concrete, start to percolate and propagate through the first-order neighbors (i.e., left, right, top, bottom) until no further progress is possible Aryanfar et al. (2019). Moving forward each new pixel is indexed in descending order. Continue the propagation until no additional progress is made and the boundary of the slump sample is reached. The computed circular region A_k is the effective slump area.

3. The difference between each successive images in the time span between the experimental images (t_k, t_{k+1}) represents the incremental area ΔA_k, which can be translated from the geometry to the incremental radius δr_k. This has been visualized in Fig. 2b.

2.3 Modeling
The obtained radius r_k from Fig. 1 is normalized to it's original value (i.e., $\frac{r(t)}{r_0}$) and it's transient behavior in time is given in Fig. 3a based on the *SAP* containment. In general the radius is time-dependent $r(t)$ and it can be could be segmented in time to obtain the values of the the radial velocity ($V_{k+1} = \frac{r_{k+1} - r_k}{\delta t}$). This gravity-driven flow generates a shear stress $\tau(t)$ proportional to the shear rate ($\dot{\gamma} = \frac{dv}{dr}$) as
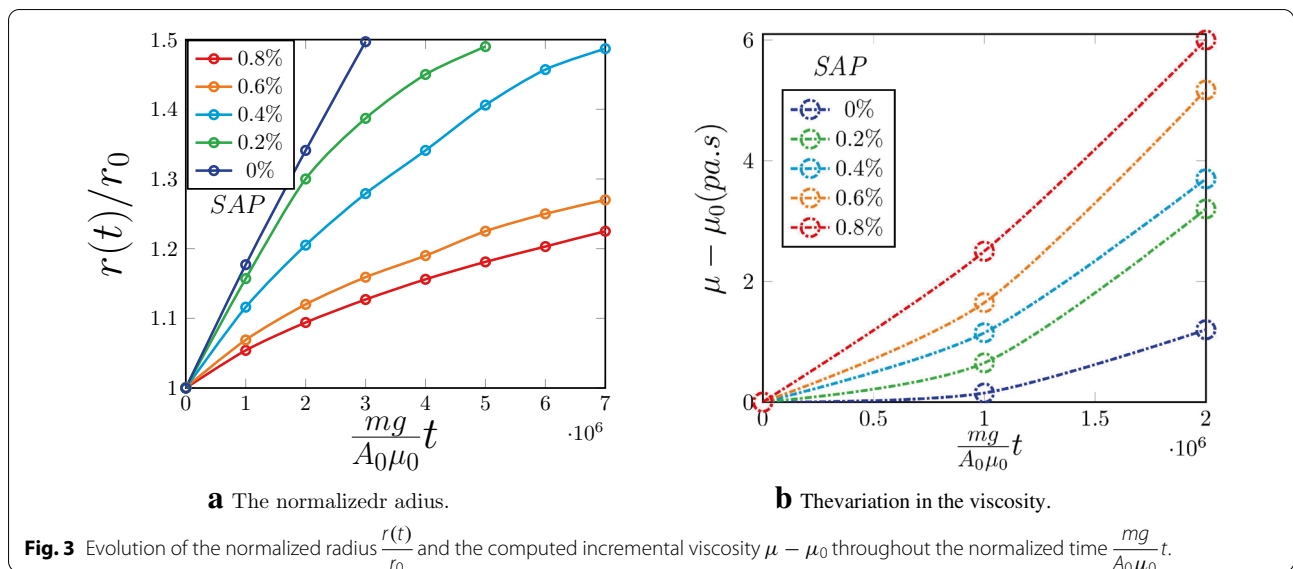
$$\tau(t) = \mu(t)\frac{dv}{dr} \tag{3}$$

where $\mu(t)$ is the instantaneous viscosity of the sample. In the absence of the external pressure gradient ($\frac{dp}{dr} \approx 0$) and the variation of the velocity in the azimuthal direction ($\frac{du}{d\theta} \approx 0$), the general Navier–Stokes relationship can be simplified as Munson (2013)

$$\rho_{mix}\left(\frac{dv}{dt} + u\frac{dv}{dr}\right) = \mu(t)\left(\frac{d^2v}{dr^2} + \frac{1}{r}\frac{\partial v}{\partial r}\right) \tag{4}$$

where the *LHS* represents the applied convective momentum applied to the sample from gravity and the *RHS* illustrates the resulted viscous momentum. Equation 4 can be solved using the finite-difference method and for simplicity the boundary of the concrete is focused-on. The boundary velocity V is defined at the given time t_k from the incremental variation in the outer radius r, such that

$$V_{k+1} = \frac{R_{k+1} - R_k}{\delta t} \tag{5}$$

a The normalizedr adius.   **b** Thevariation in the viscosity.

Fig. 3 Evolution of the normalized radius $\dfrac{r(t)}{r_0}$ and the computed incremental viscosity $\mu - \mu_0$ throughout the normalized time $\dfrac{mg}{A_0\mu_0}t$.

From Fig. 2a, the velocity value $v(r, t)$ depends on the radial distance from the center, with the boundary condition, as below:

$$\begin{cases} v(0,t) = 0 \\ v(R,t) = V \end{cases} \tag{6}$$

where u is the velocity in the boundary of the sample. Therefore, the velocity is obtained via linear approximation as

$$v(r,t) = \frac{r}{R}V(t) \tag{7}$$

Therefore, the terms in Eq. 4 are obtained as

$$\frac{dv}{dr} = \frac{1}{R}V(t)$$

and

$$\frac{d^2v}{dr^2} = 0$$

Therefore, the initial decomposition, and assuming v_i^j as the velocity in the time t^j and the radial distance r_i, adopting the scheme of forward move in time and space (*FTFS*) for segmentation of δt in time and δr in the space, Eq. 4 is discretized as

$$\rho_{mix}\left(\frac{v_i^{j+1} - v_i^j}{\delta t} + v_i^j \frac{v_{i+1}^j - v_i^j}{\delta r}\right) = \mu^j\left(\frac{1}{r_i}\frac{v_{i+1}^j - v_i^j}{\delta r}\right) \tag{8}$$

Thus, for the experimental samples in Fig. 2, the value of the viscosity μ^j is obtained as a function of *SAP*, in the given time t^j by re-arrangement as

$$\mu^j = \rho_{mix}\frac{\dfrac{v_i^{j+1} - v_i^j}{\delta t} + v_i^j \dfrac{v_{i+1}^j - v_i^j}{\delta r}}{\dfrac{1}{r_i}\dfrac{v_{i+1}^j - v_i^j}{\delta r}} \tag{9}$$

where ρ_{mix} depends on the concentration of the *SAP* utilized in the mortar mixture. If the weight concentration is α ($m_w = \alpha m_c$) the total density ρ_{mix} will be obtained as

$$\begin{aligned} \rho_{mix} &= \frac{m_{tot}}{V_{tot}} = \frac{(1+\alpha)m_c}{\dfrac{m_c}{\rho_c} + \alpha\dfrac{m_c}{\rho_w}} \\ &= (1+\alpha)\frac{\rho_w\rho_c}{\rho_w + \alpha\rho_c} \end{aligned} \tag{10}$$

where the indices w and c represent the *water* and the *cement*, respectively. Equations 9 and 5 can be merged to address the viscosity μ_k in terms of the variation in the radius r_k as below:

$$\begin{cases} \mu^j = \rho_{mix}\left(\dfrac{dv}{dt} + v\dfrac{dv}{dr}\right)\left(\dfrac{1}{r}\dfrac{dv}{dr}\right)^{-1} \\ \dfrac{dv}{dt} = \dfrac{v_i^{j+1} - v_i^j}{\delta t} \\ v\dfrac{dv}{dr} = v_i^j\dfrac{v_{i+1}^j - v_i^j}{\delta r} \\ \dfrac{1}{r}\dfrac{dv}{dr} = \dfrac{1}{r_i}\dfrac{v_{i+1}^j - v_i^j}{\delta r} \end{cases}$$

The results of computations from the above equation is shown in Fig. 3b as the difference from the original viscosity $\mu - \mu_0$, where the value of mixed density ρ_{mix} is calculated from Eq. 10. As well the normalized time is

Aryanfar *et al. Int J Concr Struct Mater*   (2021) 15:25

Page 6 of 9

shown by $\left(\dfrac{mg}{A_0\mu_0}\right)t$, where m is the mass of mortar mixture, g is gravity and A_0 and μ_0 are the initial area and viscosity of the mixture.

3 Results and Discussion

The inclusion of the higher amount *SAP* in fact means that the remaining mortar mixture is getting less workable. Despite the additional amount of water in the mixtures due to initial water absorption by the *SAP*, the slump flow decreased and the viscosity correlates directly with the *SAP* content. Meanwhile, the viscosity gain indicates that the amount of extra added water was completely absorbed by the *SAP* particles and yet still insufficient to compensate for the workability loss.

The developed image processing method in the Flowchart 1 tends to quantitatively capture such behavior via computing the incremental area A_k - and, therefore, the radius r_k - between the time slots t_k and t_{k-1}. Due to hardening behavior, such value is reduced in time as obtained in Fig. 2b, which is also obvious from the negative curvature of the normalized radius $\dfrac{r(t)}{r_0}$ versus time as shown in Fig. 3a. In fact the variation in the radius decreases with the amount of *SAP* containment, comprising the inverse effect of water absorption on the flowability Al-Nasra and Daoud (2013); Mechtcherine and Reinhardt (2012).

The finite difference computations from Eq. 3b reveals that the viscosity $\mu(t)$ is higher in the presence of augmented *SAP* mixture, therefore

$$SAP \uparrow\sim \mu \uparrow$$

which is related to the water entrainment into the SAP particles, leaving the mixtures more dry. Consequently, effect of time t is the most pronounced among all the parameters for the hardening behavior, where the viscosity is increasing exponentially. Therefore

$$t \uparrow\sim \mu \uparrow\uparrow$$

Having a closer look to the dynamics of flow in the slump test, one realizes that the radial velocity within the mortar mixture is variant. Based on Eq. 7, one gets

$$\frac{v}{V} \approx \frac{r}{R} < 1 \tag{11}$$

which means that the velocity increases linearly along the radial direction. Such velocity variation from Eq. 11 has been visualized in Fig. 4a. Since the outer-most region of the sample, with highest flowability is considered for viscosity calculation, therefore, the results show the most conservative case scenario and the viscosity in the inner regions is higher.

Viscosity results were experimentally measured for each mix by Brookfield Viscometer DV2T, as given in Fig. 4b (respective data table is available in the supplemental materials). As well the obtained rheology results for the mortar mixtures in the figure shows the direct correlation of the viscosity μ with the *SAP* concentration, the order of which is consistent with the results in Fig. 3b. While the mortar mixtures subjected to the

a Velocity distribution within the flow sample.
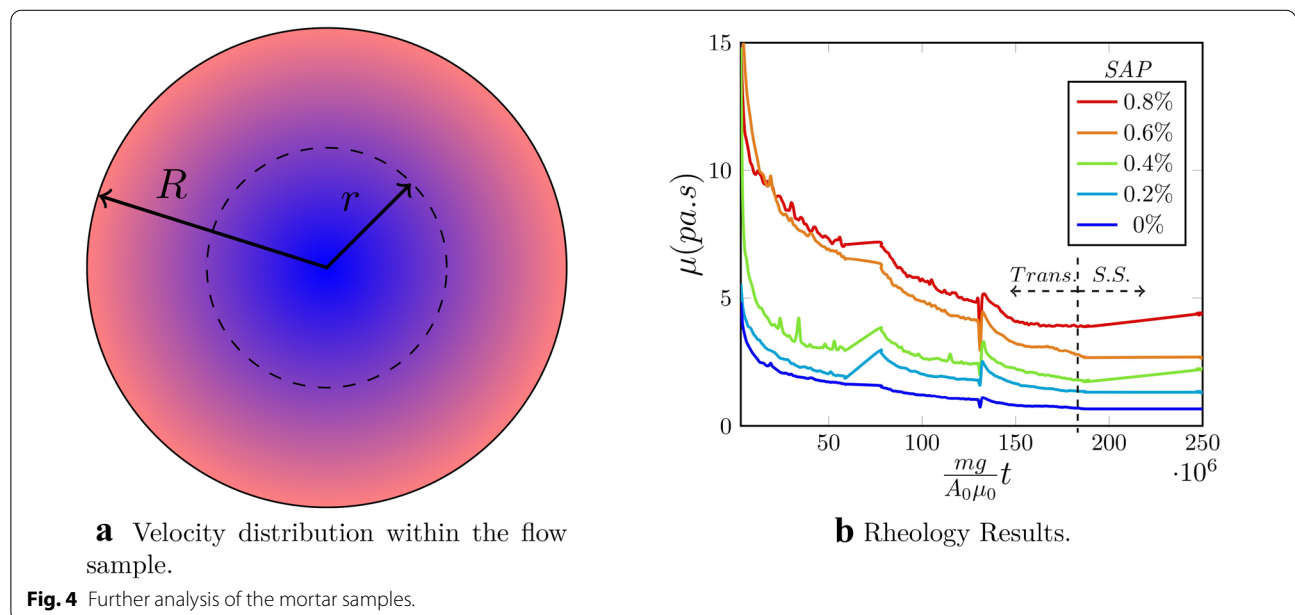

b Rheology Results.

Fig. 4 Further analysis of the mortar samples.

centrifugal force, they are initially get stretched during large deformations with high rates and reach to the stretching limit, where the obtained viscosity converges to a constant value. The transition to steady state viscosity re-emphasizes on role of the curing time during the transitory stretching of the mortar mixtures.

The comparison of the numerical result in this study with the literature in Fig. 5 reveals the increasing trend. The relative lower value of the viscosity is related to the lower containment of SAP particles ($0 - 0.8\%$ versus 10% in Hu et al. (2016)) which absorbs less amount of water, leading to more more flowable (i.e., less viscous) medium.

Ultimately, adding a certain amount of *SAP* additive per cement mass is equivalent to removing water from the concrete mix due to its water absorbency. Therefore, an decrease in slump flow spread and flow time is observed (Fig. 3a). The later-on release process of the water from SAP particles, which can occur during the long run, leads to a formation of moisturized concrete with a fraction of water containment W. In such case, the viscosity of the mixture μ_{mix} is described from classic theory as LaAHN (1949)

$$\log \mu_{mix} = N_c \log \mu_c + N_w \log \mu_w \quad (12)$$

where N_c and N_w and μ_{ct} and μ_w represent the mole fraction and the viscosity for cement and water, respectively. The mole fraction N is defined as

$$N_c = \frac{n_c}{n_c + n_w}$$
$$= \frac{\dfrac{m_c}{M_c}}{\dfrac{m_c}{M_c} + \dfrac{m_w}{M_w}}$$

where n_c and n_w and m_c and m_w and M_c and M_w are the number of moles, the respective mass and the molar mass of cement and water, respectively. Based on the release process, one has

$$W = \frac{m_w}{m_c + m_w}$$

solving for the mass of cement m_c one has

$$m_c = m_w \left(\frac{1 - W}{W} \right)$$

the mole fraction of the cement N_c is obtained consequently as

$$N_c = \frac{(1 - W)M_W}{WM_c + (1 - W)M_w}$$

and, respectively, the mole fraction of water N_w is obtained as

$$N_w = \frac{WM_c}{WM_c + (1 - W)M_w}$$

Hence, the mixed viscosity μ_{mix} is obtained subsequently as

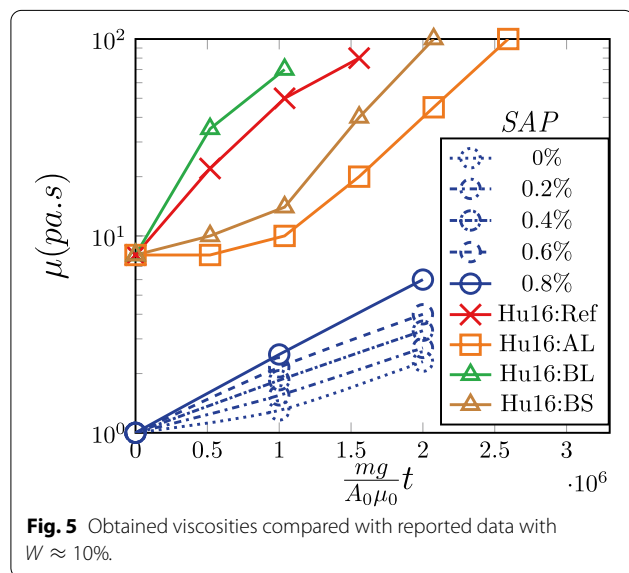$$\mu_{mix} = \exp \left(\frac{WM_W}{WM_w + (1 - W)M_c} \log \mu_c + \frac{(1 - W)M_c}{WM_w + (1 - W)M_c} \log \mu_w \right) \quad (13)$$

which is in fact an Arrhenius-type relationship Arrhenius (1887). In fact such exponential trend resonates very well with the obtained viscosity results in Fig. 3b and the linear trend obtained in the log scale in Fig. 5.

4 Conclusions

In this paper, an image-processing method has been developed as a powerful technique for computing the radial propagation, the velocity and ultimately the instantaneous viscosity of the mortar mixtures with the given concentration of the super absorbent polymer. While the method, which is supported by the supplemental rheological measurement and analytical elaboration, can be used for predicting the concrete's workability before casting process, the quantified utilization of SAP contents can be used as determining parameters to tune the other flow properties of the concrete effectively. Further studies are on the way for characterizing the combination of SAP

Fig. 5 Obtained viscosities compared with reported data with $W \approx 10\%$.

Aryanfar *et al. Int J Concr Struct Mater*   (2021) 15:25

Page 8 of 9

with superplasticizer (*SP*) on the fresh state rheological properties of cementitious mortars.

Authors' contributions
AA: conceptualization, validation, formal analysis, investigation, data curation, writing original/final draft, writing—review/editing, visualization. IS: experimentation, writing—review/editing, formal analysis, and data curation. JM: supervision and project administration. All authors read ad approved the final manuscript.

Authors' informations
Asghar Aryanfar is Assistant Professor of Mechanical Engineering at American University of Beirut. He received PhD from California Institute of Technology, Pasadena, CA in 2015 and his research is on the multi-physical modeling of nonlinear events in heterogenous media.

Irem Şanal is Assistant Professor of Civil Engineering at Bahcesehir University, Istanbul, Turkey. She received her PhD from Bogazici University and her research is on fibre reinforced and sustainable concrete, crack monitoring, and environmental impacts.

Jaime Marian is Associate Professor of Material Science and Mechanical Engineering at University of Califorinia, Los Angeles (UCLA). His research interest is Computational Material Science and Solid Mechanics.

Availability of data and materials
The processed data required to reproduce these findings are available to download from http://dx.doi.org/10.17632/7r2ckfp45h.2.

Declarations

Competing interests
The authors declare no competing financial interest regarding this publication.

Author details
[1]American University of Beirut, Riad El-Solh 1107 2020, Lebanon. [2]Bahçeşehir University, 4 Çırağan Cad, Beşiktaş, Istanbul 34353, Turkey. [3]University of California, 400 Westwood Plaza, Los Angeles, CA 90095, USA.

References
Grunberg, L. A., & Nissan, A., F. Mixture law for viscosity. *Nature*, 164(4175):799–800, 1949.

Al-Nasra, M., & Daoud, M. (2013). Investigating the use of super absorbent polymer in plain concrete. *International Journal of Emerging Technology and Advanced Engineering, 3*(8), 598–603.

Arrhenius, S. (1887). Über die innere reibung verdünnter wässeriger lösungen. *Zeitschrift für Physikalische Chemie, 1*(1), 285–298.

Aryanfar, A., Hoffmann, M. R., & William, A. (2019) . Finite-pulse waves for efficient suppression of evolving mesoscale dendrites in rechargeable batteries. *Physical Review E*, 100(4):042801, 2019.

Aryanfar, A., Goddard III, W., & Marian, J. (2019) Constriction percolation model for coupled diffusion-reaction corrosion of zirconium in pwr. *Corrosion Science*, 158:108058,

AzariJafari, H., Kazemian, A., Rahimi, M., & Yahia, A. (2016). Effects of pre-soaked super absorbent polymers on fresh and hardened properties of self-consolidating lightweight concrete. *Construction and Building Materials, 113*, 215–220.

Craeye, B., & De Schutter, G. (2008) Experimental evaluation of mitigation of autogenous shrinkage by means of a vertical dilatometer for concrete. In *Eight International Conference on Creep, Shrinkage and Durability Mechanics of Concrete and Concrete Structures*, pages 909–914. CRC Press/Balkema

Dudziak, L., & Mechtcherine, V. (2010). Enhancing early-age resistance to cracking in high-strength cement based materials by means of internal curing using super absorbent polymers. *RILEM Proc. PRO, 77*, 129–139.

Dudziak, L., & Mechtcherine, V. (2009) . Reducing the cracking potential of ultra high performance concrete by using super absorbent polymers (sap). In *Proceedings of the International Conference on Advanced Concrete Materials (ACM 09)*, pages 11–19

Esteves, L. P. (2011). Superabsorbent polymers: On their interaction with water and pore fluid. *Cement and concrete composites, 33*(7), 717–724.

Han, J., Fang, H., & Wang, K. (2014). Design and control shrinkage behavior of high-strength self-consolidating concrete using shrinkage-reducing admixture and super-absorbent polymer. *Journal of sustainable cement-based materials, 3*(3–4), 182–190.

Hu, Q., Yamazaki, K., & Igarashi, S. (2016) Kinetics of water absorption and desorption of superabsorbent polymers and its effect on plastic viscosity of cement paste at early age. volume 38. CRC Press/Balkema

Igarashi, S., & Watanabe, A. (2006) Experimental study on prevention of autogenous deformation by internal curing using super-absorbent polymer particles. In *International RILEM conference on volume changes of hardening concrete: testing and mitigation*, pages 77–86. RILEM Publications SARL Lyngby

Jensen, O. M., & Hansen, P. F. (2001) Water-entrained cement-based materials: I. principles and theoretical background. *Cement and concrete research*, 31(4):647–654

Jensen, O. M., & Hansen, P. F. (2002) Water-entrained cement-based materials: Ii. experimental observations. *Cement and Concrete Research*, 32(6):973–978

Justs, J., Wyrzykowski, Mateusz, Bajare, Diana, & Lura, Pietro. (2015). Internal curing by superabsorbent polymers in ultra-high performance concrete. *Cement and Concrete Research, 76*, 82–90.

Kong, X., & Zhang, Z. (2013). Effect of super-absorbent polymer on pore structure of hardened cement paste in high-strength concrete. *Journal of the Chinese Ceramic Society, 41*(11), 1474–1480.

Kong, X., & Zhang, Z. (2014). Shrinkagereducing mechanism of superabsorbent polymer in highstrength concrete. *Journal of the Chinese Ceramic Society, 42*(2), 150–155.

Lee, H. X. D., Wong, H. S., & Buenfeld, N. R. (2016). Self-sealing of cracks in concrete using superabsorbent polymers. *Cement and concrete Research, 79*, 194–208.

Mechtcherine, V., Secrieru, E., & Schrofl, C. (2015). Effect of superabsorbent polymers (saps) on rheological properties of fresh cement-based mortars development of yield stress and plastic viscosity over time. *Cement and Concrete Research, 67*, 52–65.

Mechtcherine, V., & Reinhardt, H. (2012) . *Application of super absorbent polymers (SAP) in concrete construction: state-of-the-art report prepared by Technical Committee 225-SAP*, volume 2. Springer Science & Business Media

Mechtcherine, V., Dudziak, L., Schulze, J., & Staehr, H. (2006) . Internal curing by super absorbent polymers (sap)–effects on material properties of self-compacting fibre-reinforced high performance concrete. In *Int RILEM Conf on Volume Changes of Hardening Concrete: Testing and Mitigation, Lyngby, Denmark*, pages 87–96

Mejlhede Jensen, O. (2013). Use of superabsorbent polymers in concrete. *Concrete international, 35*(1), 48–52.

Munson, B. R. (2013). *Theodore Hisao Okiishi, Wade W Huebsch, and Alric P Rothmayer*. Wiley Singapore: Fluid mechanics.

Otsu, N. (1975). A threshold selection method from gray-level histograms. *Automatica, 11*(285–296), 23–27.

Paiva, H., Esteves, L. P., Cachim, P. B., & Ferreira, V. M. (2009). Rheology and hardened properties of single-coat render mortars with different types of water retaining agents. *Construction and Building Materials, 23*(2), 1141–1146.

Paiva, H., Silva, L. M., Labrincha, J. A., & Ferreira, V. M. (2006). Effects of a water-retaining agent on the rheological behaviour of a single-coat render mortar. *Cement and Concrete Research, 36*(7), 1257–1262.

Pang, L., Feng, R., Shi Y., & Cai, Y. T. (2011) . Effects of internal curing by super absorbent polymer on shrinkage of concrete. In *Key Engineering Materials*, volume 477, pages 200–204. Trans Tech Publ

Popovics, S. (1998). *Strength and related properties of concrete: a quantitative approach*. New York, Wiley.

Powers, T. C., & Brownyard, T. L. (1946). Studies of the physical properties of hardened portland cement paste. *Journal Proceedings, 43,* 101–132.

Schröfl, C., Mechtcherine, V., & Gorges, M. (2012). Relation between the molecular structure and the efficiency of superabsorbent polymers (sap) as concrete admixture to mitigate autogenous shrinkage. *Cement and Concrete Research, 42*(6), 865–873.

Shen, D., Wang, T., Chen, Y., Wang, M., & Jiang, G. (2015). Effect of internal curing with super absorbent polymers on the relative humidity of early-age concrete. *Construction and Building Materials, 99,* 246–253.

Toledo, F., Romildo D., Silva, E. F., Lopes, Anne NM., Mechtcherine, V., & Dudziak, L. (2012) . Effect of superabsorbent polymers on the workability of concrete and mortar. In *Application of Super Absorbent Polymers (SAP) in Concrete Construction*, pages 39–50. Springer

Wang, F., Zhou, Y., Peng, B., Liu, Z., & Shuguang, H. (2009). Autogenous shrinkage of concrete with super-absorbent polymer. *ACI Materials Journal, 106*(2), 123.

Publisher's Note